ELSEVIER

Materials Science and Engineering C 8–9 (1999) 309–318

MATERIALS SCIENCE & ENGINEERING C

www.elsevier.com/locate/msec

Synthesis of nanoparticles in Langmuir monolayer

G.B. Khomutov [a,*], A.Yu. Obydenov [a], S.A. Yakovenko [a], E.S. Soldatov [a], A.S. Trifonov [a], V.V. Khanin [a], S.P. Gubin [b]

[a] *Faculty of Physics, M.V. Lomonosov Moscow State University, 119899 Moscow, Russian Federation*
[b] *Institute of General and Inorganic Chemistry RAS, 119899 Moscow, Russian Federation*

Abstract

A novel approach to create ultrathin planar nanoparticulate structures based on the controllable synthesis of nanoparticles directly in Langmuir monolayer at the gas/liquid interface and subsequent deposition of monolayer is introduced. In this approach, all initial reagents are present only in monolayer and reactions of nanoparticles synthesis are initiated by decomposition of organometallic compounds under electromagnetic radiation. The changes in the shape of compression isotherm of stearic acid (SA)/iron pentacarbonyl mixed monolayer under the varying of the time of exposure to the ultraviolet light have been studied. STM images of mixed monolayers deposited onto the graphite substrate revealed synthesized iron isotropic and anisotropic magnetic nanoparticles with the characteristic size varied from 20 to 150 Å in dependence on the ultraviolet exposure time and monolayer compression.

Keywords: Monolayer; Nanoparticles; Synthesis; STM

1. Introduction

Materials with monodispersed metallic nanoparticles in a solid or liquid matrix often possess new properties, important and perspective for wide applications. A number of methods to prepare ultrafine particles were developed up to now and were exploited to create different particulate materials as, for example, ferrofluids and metallopolymers [1,2].

Langmuir–Blodgett (LB) technique allows to create multicomponent organized ultrathin molecular films with incorporated or grown inside clusters and nanoparticles, what is very promising new material for nanotechnology, molecular electronics, optic systems, catalysis and coatings with controlled properties. This approach allows the formation of planar nanoparticulate structures of ultimately small thickness, corresponding to the dimensions of single nanoparticle monolayer plane, and to create corresponding multilayer nanoparticle-containing structures of strictly controllable thickness, determined by a number of deposited nanoparticulate monolayers. We have exploited this technique to fabricate mixed monolayer LB films consisted of inert amphiphile molecular matrix and guest organometallic clusters to create the reproducible stable planar nanostructures with different systems of electron tunnel junctions [3]. The double tunnel junction (DTJ) structure ''graphite substrate–cluster–STM tip'' was studied [4,5] and corresponding molecular single electron tunneling (SET)-transistor was demonstrated at room temperature [6].

The nanoparticulate LB films were formed as a rule in two ways; first, with the use of ultrafine particles prepared prior to their incorporation into the film [7–10]. In another method, nanoparticles were generated within or at the interfaces of surfactant monolayers used as templates [11–13] or inside LB films of fatty acid salts and another surfactants [14–17]. When Langmuir monolayer served as template for synthesis of nanoparticles, the initial reagents were located in a gas and/or liquid phases.

It is known that ultrafine metallic particles can be prepared by decomposition of organometallic compounds such as transition metal carbonyls. The decomposition is caused by introducing sufficient energy into the molecule to cause bond scission. This can be done mechanically, thermally or by electromagnetic radiation. Thus, ferroflu-

* Corresponding author. Tel.: +7-95-132-2418; fax: +7-95-939-1195; E-mail: gbk@bio383a.phys.msu.su

0928-4931/99/$ - see front matter
PII: S0928-4931(99)00026-0

ids consisting of colloidal suspensions of stabilized metallic nanoparticles were prepared by thermal or ultraviolet irradiation decomposition of transition metal carbonyls in presence of surfactant [18–24].

We report here the synthesis of iron magnetic nanoparticles directly in Langmuir monolayer at the gas/liquid interface when all initial reagents are present only in monolayer. The nanoparticles were formed by the ultraviolet decomposition of an iron pentacarbonyl present in monolayer in a sufficient amount to form a substantial number of particles per area at the gas/liquid interface in the presence of monolayer molecular surfactant matrix (stearic acid, SA). Iron pentacarbonyl and mixed SA/iron pentacarbonyl Langmuir monolayers behavior on the water surface have been studied in dependence on the time of exposure to the ultraviolet light. The microtopography of nanoparticulate monolayer deposited and effects of SET were studied using STM technique at room temperature. Our STM study reveals that through the systematic control of the ultraviolet irradiation dose and of the mixed monolayer content and compression extent one can manipulate the growth process of nanoparticles and deposit two-dimensional (2-D) ordered nanoparticulate structures. The effects related to SET and energy quantization of electrons were observed in formed planar nanoparticulate molecular structures.

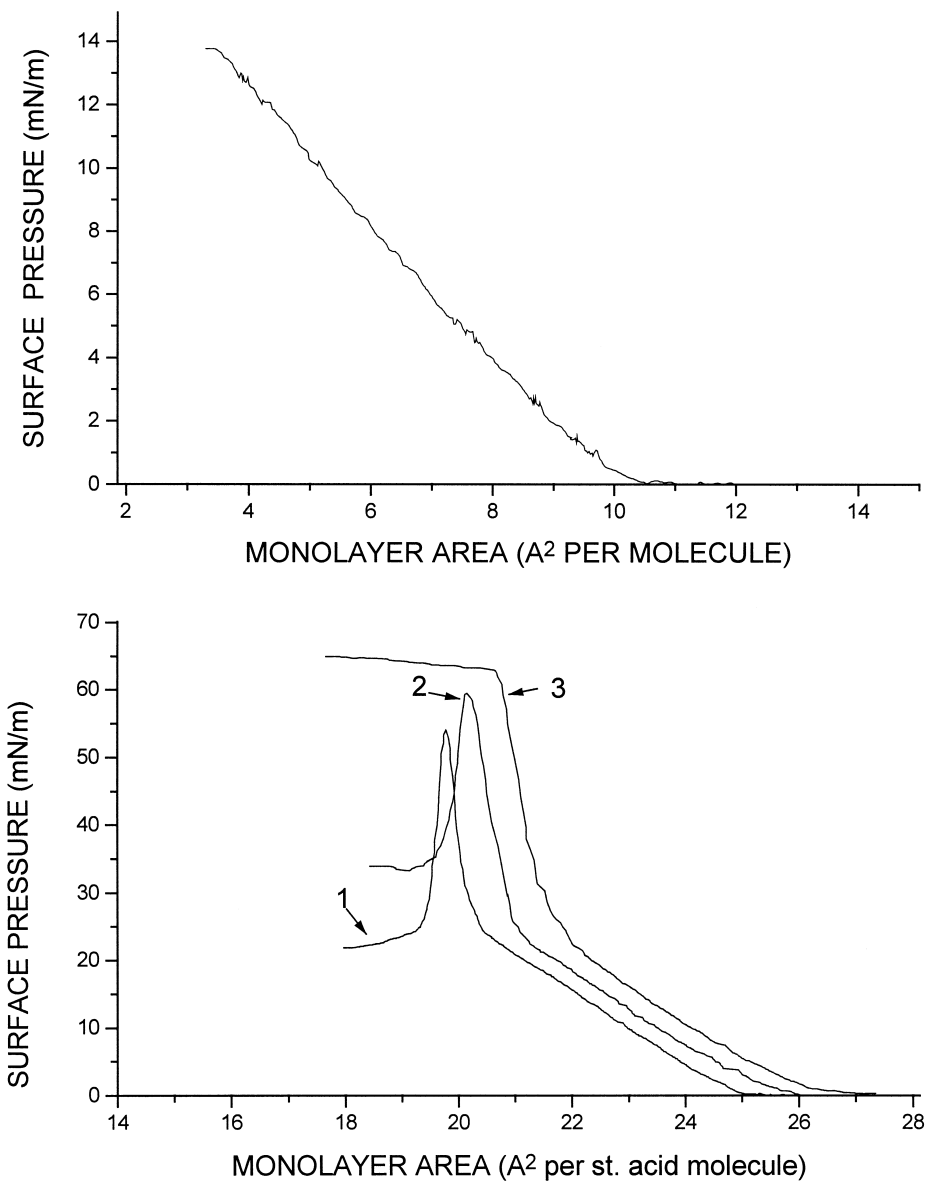

Fig. 1. (a) The *P–A* isotherm of pure iron pentacarbonyl on water subphase. (b) The *P–A* isotherms of mixed Langmuir monolayers consisted of SA and iron pentacarbonyl on water subphase. Curve 1: control monolayer of pure SA; curve 2: mixed monolayer ($Fe(CO)_5$/SA ratio 20:1), compression in the dark without ultraviolet irradiation; curve 3: mixed monolayer ($Fe(CO)_5$/SA ratio 20:1), compression after 3 min exposure to ultraviolet light. Monolayer area is calculated per molecule of SA. Water subphase pH = 5.6. T = 295 K.

2. Materials and methods

SA (CH_3–$(CH_2)_{16}$–COOH) was obtained from Serva. Iron pentacarbonyl $Fe(CO)_5$ was obtained from Alfa Inorganic and used without further purification. Water was purified by a Milli-Q system (Millipore).

Surface pressure–monolayer area (P–A) isotherm measurements and monolayer transfer to solid substrates were carried out on a full automatic conventional teflon trough at 18–20°C as described elsewhere [25]. Langmuir monolayers were formed by spreading a mixed chloroform solution of $Fe(CO)_5$ with SA 2×10^{-4} M on the surface

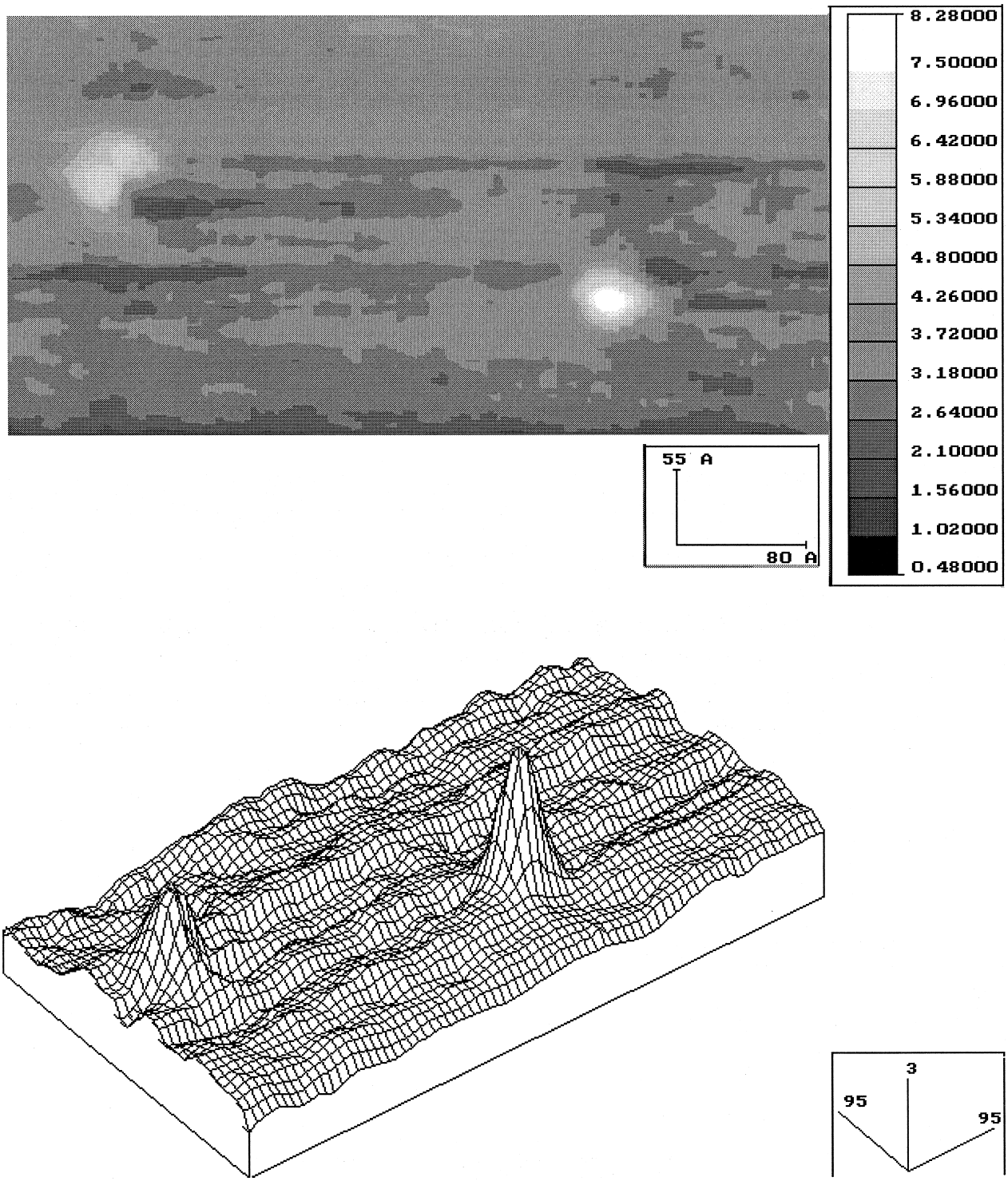

Fig. 2. STM topographic images of mixed nanoparticulate monolayers ($Fe(CO)_5$/SA ratio 20:1, 3 min exposure to ultraviolet light, surface pressure under illumination ~ 1 mN/m) deposited by Shaefer's method onto the surface of graphite substrate. (a) Top view; (b) 3-D image. The scales of images are shown in the right bottom corner of pictures. $T = 295$ K.

of purified water (pH = 5.6). After complete solvent evaporation, the floating monolayer was compressed by a mobile Teflon barrier at a speed ~ 3 A^2/SA molecule min to different compression extent. The $Fe(CO)_5$ evolves carbon monoxide when exposed to heat or light. Mixed $Fe(CO)_5$/SA monolayer ($Fe(Co)_5$/SA ratio varied from 50:1 to 1:1) was irradiated by ultraviolet light for different time intervals using 100 mW conventional IVR ultraviolet light source ($\lambda = 300$ nm). Monolayers were then compressed and deposited onto high oriented pyrolytic graphite (HOPG) substrate at a constant pressure (25 mN/m), temperature and dipping speed using the conventional horizontal lifting method with good transfer ratios, to form monolayer nanoparticulate samples for STM investigations. Multilayer nanoparticle-containing Y-type LB films were formed by means of vertical lifting deposition onto polished silicon substrates with natural oxide layer at surface pressure 25 mN/m. The electron paramagnetic resonance (EPR) technique was used to study the magnetic properties of nanoparticulate multilayer LB films. The EPR spectra were recorded with Varian E-4 spectrometer at the X band at room temperature.

The STM measurements of the monolayer films deposited on a HOPG surface were performed using a modified Nanoscope-1 scanning tunneling microscope in the constant current mode. Topographic images of the films were measured usually at tip bias voltage 0.5 V and tunneling current 0.5 nÅ. The images were stable and reproducible. The formed planar nanoparticulate molecular structures were studied spectroscopically by recording tunneling current–bias voltage (I–V) curves in DTJ geometry, where nanoparticles were coupled via two tunnel junctions to two macroscopic electrodes (HOPG substrate and the tip of a STM). The measurement procedure consisted of the obtaining of topographic image and then positioning the tip above an isolated nanoparticle for the tunneling spectroscopy measurements. I–V curves were recorded while temporarily disconnecting the feedback circuit and, therefore, with constant tunnel junctions parameters. During the I–V measurements, topographic images were monitored regularly to ensure that the tip and the nanoparticle not drift apart. Electrons flowed from the tip to the substrate for positive V values.

3. Results and discussion

3.1. Surface P–A isotherms

Long-chain fatty acids and their derivatives are known as classical surfactant compounds to form insoluble monolayers at the water/air interface [26]. Using those compounds, high ordered LB films were formed perspective for device applications in several diverse areas including solid state molecular electronics, nanolithography, and different kinds of sensors [27]. Simultaneously, such compounds are widely used as surfactants to stabilize nanoparticles in nanoparticulate materials, for example, in magnetic paints and ferrofluids [28]. In our approach, the properties of fatty acids to form Langmuir monolayer and to stabilize nanoparticles and prevent aggregation in nanoparticulate structures are combined successfully.

Iron pentacarbonyl and mixed SA/iron pentacarbonyl Langmuir monolayers behavior on the water surface have been studied in dependence on the time of exposure to the ultraviolet light. Fig. 1a shows the P–A isotherm of pure iron pentacarbonyl on the surface of water subphase. It is clear from this figure that iron pentacarbonyl possess surfactant properties. We have prepared mixed Langmuir monolayers consisted of SA and iron pentacarbonyl in different ratios and studied compression isotherm changes in dependence on monolayer content and on the period of ultraviolet light irradiation. Fig. 1b shows the compression isotherms of control SA and mixed monolayers on water subphase at 20°C. The course of P–A isotherm of control pure SA monolayer without iron pentacarbonyl (showed on curve 1 of Fig. 2) was not changed noticeably after ultraviolet light irradiation during 25 min. The dark compression isotherm of mixed monolayer ($Fe(CO)_5$/SA ratios was varied from 50:1 to 1:1) without ultraviolet irradiation was usually shifted to the large monolayer areas in comparison with control. The typical dark P–A isotherm of monolayer with $Fe(CO)_5$/SA ratio 20:1 is presented in Fig. 1b (curve 2). The characteristic compression isotherm of mixed SA/iron pentacarbonyl monolayer exposure to ultraviolet light is shown in Fig. 1b, curve 3. P–A isotherms in this case were characterized by suppression of phase transitions, change in collapse behavior and significant increase in A_o (value of monolayer area where P began to increase from 0) in comparison with control. Those changes give evidence that monolayer structure and intermolecular interactions are substantially altered by nanoparticles synthesized under ultraviolet illumination.

3.2. STM measurements

STM have been advantageously used to study microtopography of surface and electron transport processes in molecular and nanoparticulate planar systems [5,12,29]. Molecular structure of samples for investigations of single nanoparticles by this technique has to be monolayer on the conducting substrate. STM image of pure SA monolayer,

Fig. 3. STM topographic images of mixed nanoparticulate monolayers ($Fe(CO)_5$/SA ratio 20:1, 3 min exposure to ultraviolet light, surface pressure under illumination ~ 7 mN/m) deposited by Shaefer's method onto the surface of graphite substrate. (a) Top view; (b) 3-D image. The scales of images are shown in the right bottom corner of pictures. $T = 295$ K.

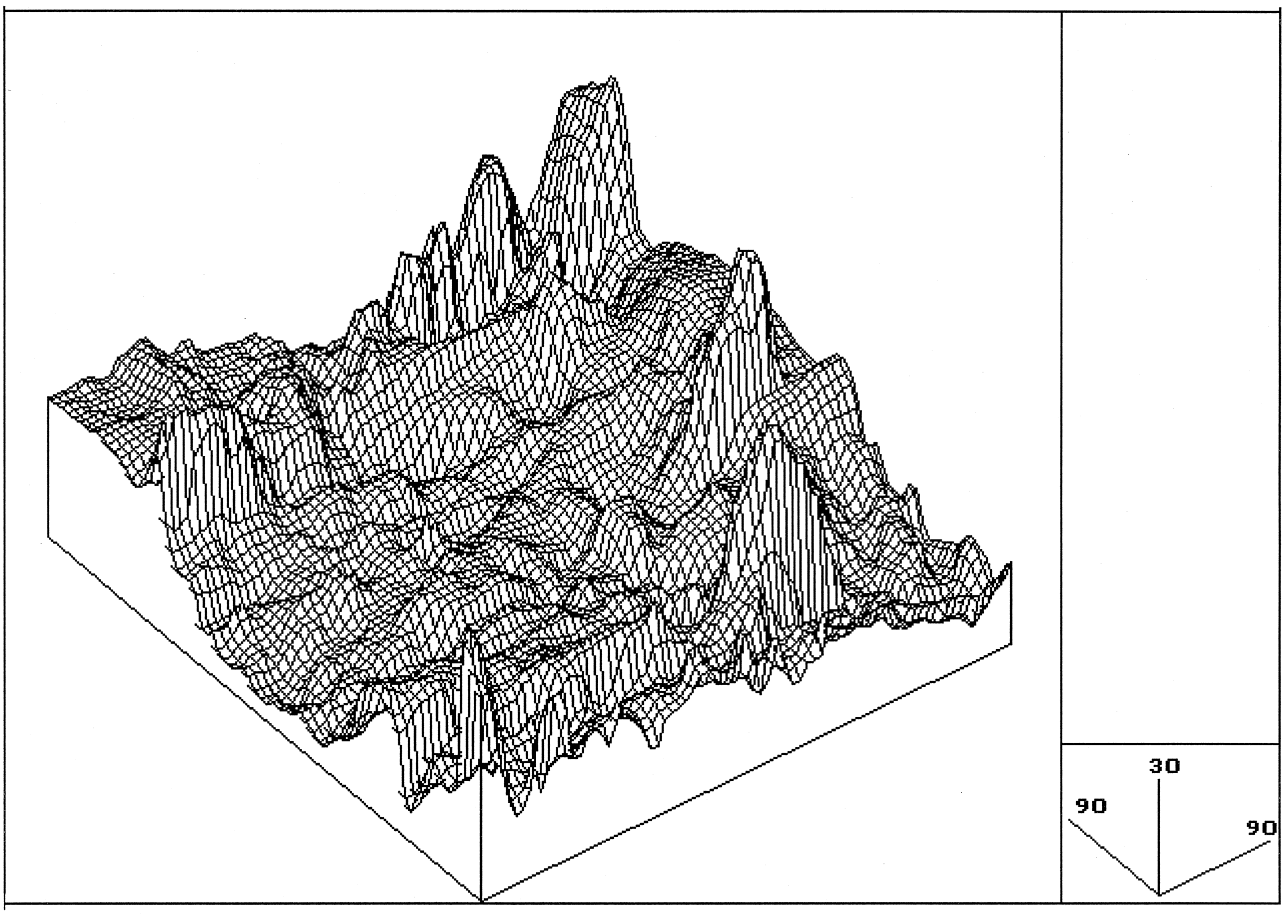
30
90
90

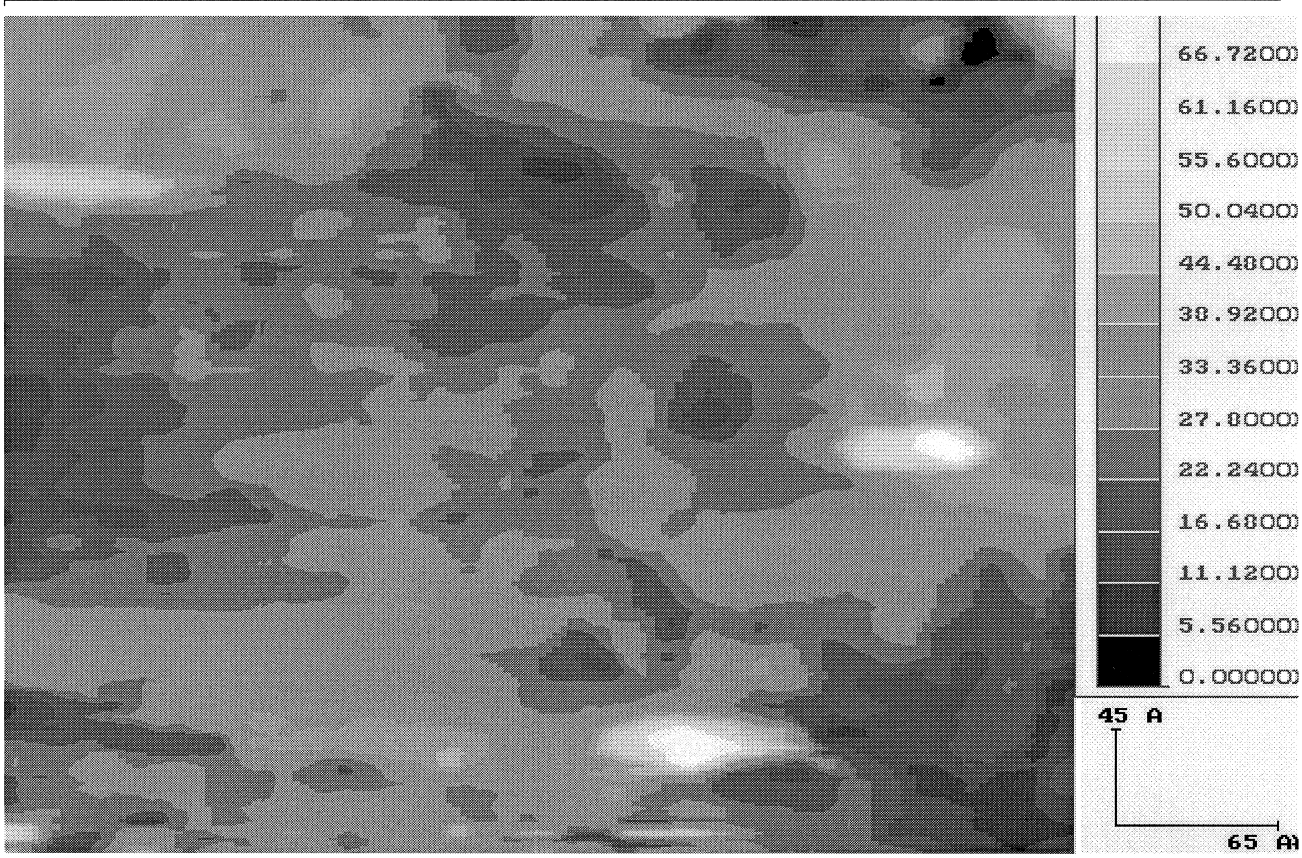
66.7200
61.1600
55.6000
50.0400
44.4800
38.9200
33.3600
27.8000
22.2400
16.6800
11.1200
5.56000
0.00000
45 A
65 A

transferred to a graphite substrate from the surface of aqueous phase by horizontal lifting method, is a quasi-planar and very smooth surface without any 3-D structures included [12]. The mixed monolayers containing synthe-

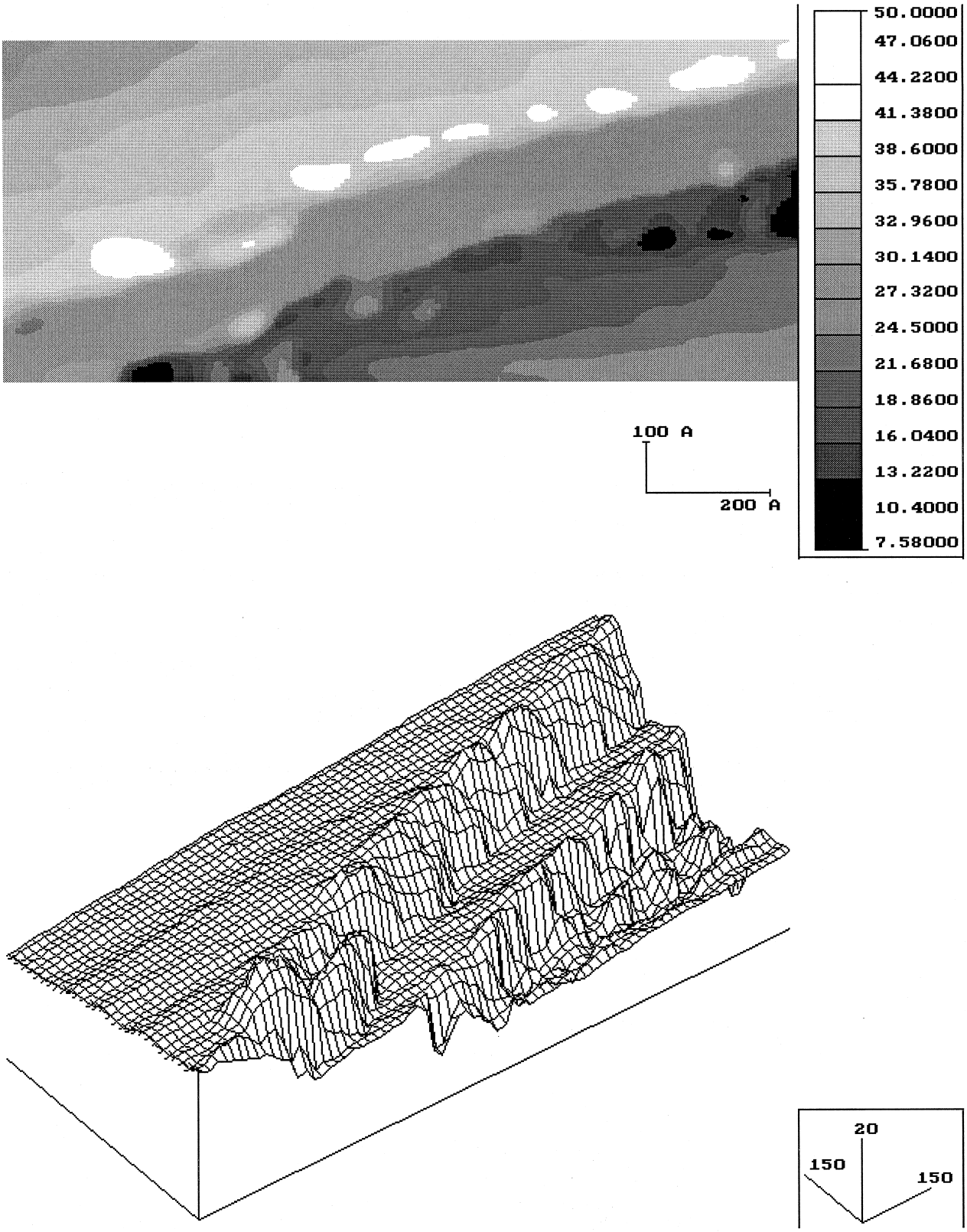

Fig. 4. STM topographic images of mixed nanoparticulate monolayers ($Fe(CO)_5$/SA ratio 20:1, 10 min exposure to ultraviolet light, surface pressure under illumination ~ 1 mN/m) deposited by Shaefer's method onto the surface of graphite substrate. (a) Top view; (b) 3-D image. The scales of images are shown in the right bottom corner of pictures. $T = 295$ K.

sized nanoparticles were successfully deposited onto HOPG substrate using Shaefer's method. STM topographic images of different mixed ultraviolet irradiated monolayers deposited onto the HOPG substrate revealed synthesized iron nanoparticles and aggregates. The particle size depended significantly on the mixed monolayer exposure time to the ultraviolet light. Fig. 2 represents characteristic STM images of nanoparticulate monolayer (initial $Fe(CO)_5/SA$ ratio was 20:1) deposited after 3 min irradiation by ultraviolet light at surface pressure ~ 1 mN/m. The STM microtopographic images in this case revealed the formation of small (~ 2 nm size) isotropic platelike nanoparticles. The size and the shape of nanoparticles were reproducible and nanoparticles were usually homogeneously distributed in monolayer. The compression of monolayer of the same content under ultraviolet illumination resulted in formation of anisotropic ellipsoid-like nanoparticles (Fig. 3). In monolayers ($Fe(CO)_5/SA = 20:1$) deposited after 10 min ultraviolet irradiation, single nanoparticles and ordered groups of particles were also observed. Fig. 4 shows the chain of nanoparticles typically observed in such monolayer. It is known that particles with dipole moment aggregate into chains when dipole–dipole interaction energy exceeds k_BT (k_B: Boltzmann constant). Chains of magnetic ultrafine particles are usually observed in magnetic liquids [1,28] and it gives evidence that iron nanoparticles synthesized in our experiments have noticeable magnetic moment. The increase of the time of monolayer exposure to ultraviolet light or increase of the iron pentacarbonyl content in monolayer (above 30 for $Fe(CO)_5/SA$ ratio) resulted in formation of some random iron aggregative structures typical one as shown in Fig. 5.

The results presented are in agreement with those obtained previously on decomposition of $Fe(CO)_5$ in liquids chemically close to SA [30,31]. It was found that all nanoparticles formed were multiphase, the major phase was α-Fe, some types of iron oxides and iron carbide were present [31]. It was found that in 3-D media after nucleation of an iron particle, it grows very rapidly to a size large than 4.5 nm [32]. It was shown that the particle size depends on the type of surfactant molecules used and in the absence of a surfactant the particle size exceeds 100 nm and the strong total intensive aggregation of particles occurred [32].

The room temperature tunnel current–voltage (I–V) dependencies recorded using STM on the small nanoparticle (~ 2 nm) revealed effects related to single-electron tunneling and, possibly, energy quantization of electrons in DTJ structures. Corresponding spectroscopic results, namely, the I–V and dI/dV characteristics are shown in Fig. 6a,b. The curves with pronounced Coulomb-blockade region near zero voltage were observed only on the

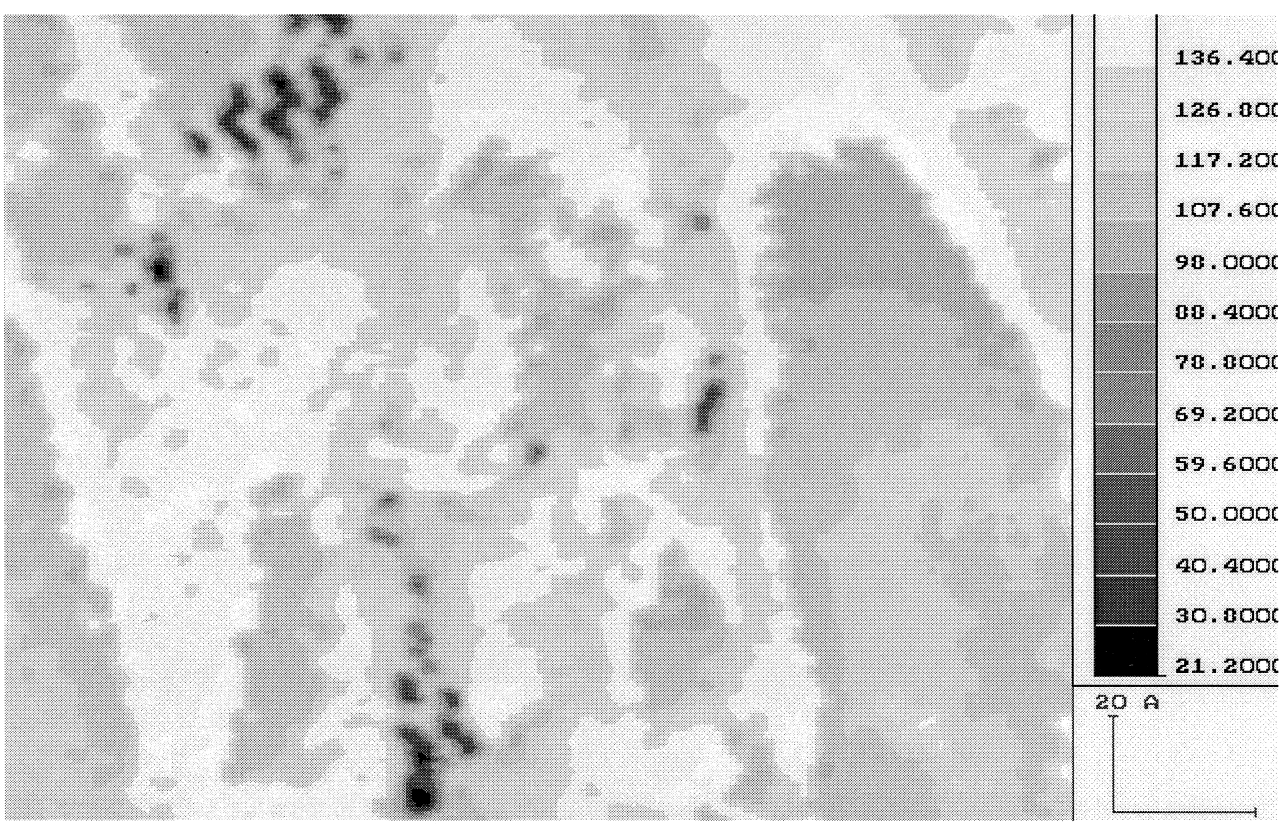

Fig. 5. STM topographic images of mixed nanoparticulate monolayers ($Fe(CO)_5/SA$ ratio 20:1, 30 min exposure to ultraviolet light, surface pressure under illumination ~ 1 mN/m) deposited by Shaefer's method onto the surface of graphite substrate. (a) Top view; (b) 3-D image. The scales of images are shown in the right bottom corner of pictures. $T = 295$ K.

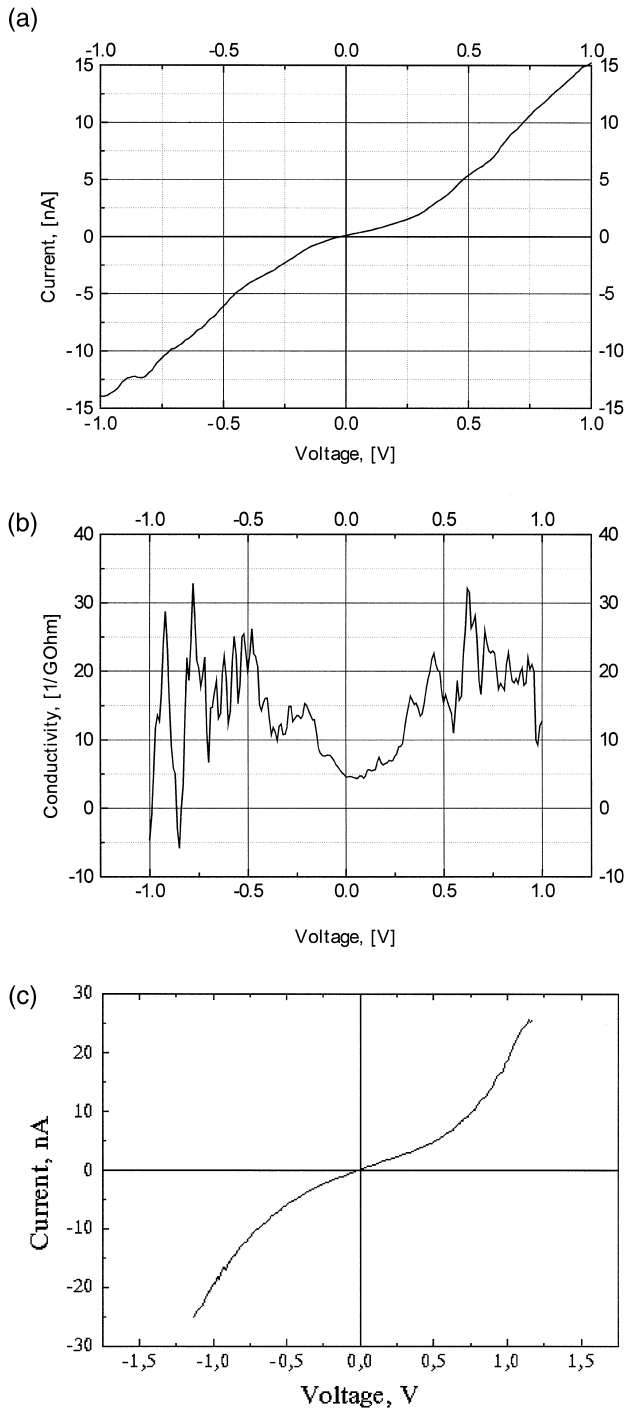

Fig. 6. STM tunneling current–voltage ($I-V$) characteristics of nanoparticulate mixed monolayer recorded in DTJ system ''STM tip–monolayer–graphite substrate'' at 295 K. (a) Characteristic $I-V$ curve recorded when the tip was positioned on the nanoparticle; (b) tunneling spectroscopic dI/dV curve corresponding to curve (a); (c) typical $I-V$ curve recorded on the mixed monolayer surface area without nanoparticles and on the SA monolayer.

nanoparticles, whereas identical smooth $I-V$ curves without noticeable particular features (Fig. 6c) were obtained everywhere else except over the nanoparticles. The $I-V$ curve shown in Fig. 6c is characteristic for SA monolayer onto graphite substrate and its super linear course is usual for single tunnel junctions ''STM tip–substrate'' [33]. The $I-V$ curve in Fig. 6a is determined by the tunnel junctions parameters, the energy separation of highest occupied molecular orbital (HOMO) and the lowest unoccupied molecular orbital (LUMO) in nanoparticle and its combination with Coulomb single-electron charging effects during tunneling. The $I-V$ picture can be complicated also by molecular orbital anisotropy when tunneling current is correspondingly dependent on the tip position over the particle and on the nanoparticle space orientation with respect to the substrate surface. The curves with suppressed conductivity near zero voltage (the typical one shown in Fig. 6a may be interpreted as a result of single-electron tunneling in DTJ system ''STM tip–nanoparticle–substrate''. The size of the nanoparticle is about 2 nm and the capacitance of each tunnel junction can be estimated as 0.1 aF (10^{-19} F) [4]. This value gives the Coulomb blockade region about 0.3 V which is close to the experimental value (Fig. 6a). These facts give evidence that the steps on the $I-V$ curves may be due to the SET effects.

The single electron charging effects and quantum size effects in isolated conducting nanoparticles are of principal importance in development of nanoscale functional systems (including quantum functional elements and devices). Each of these effects can be detected when charging energy and/or electronic level separation exceed the thermal energy k_BT. The manifestation of both effects correlates as a rule with decrease in nanoparticle size. Our data give evidence that the described approach can be used in development of high temperature SET systems. Concerning electron tunneling in constructed tunnel junctions of superparamagnetic ultrafine particles, one would expect also manifestations of magnetotunneling effects in dependence of external magnetic field and interactions of magnetic moments of particles.

3.3. EPR measurements

Because of very small magnetic moment of ultrathin LB film formed, it is hardly possible to register directly the magnetization curve in these samples. EPR spectroscopy has been actively used as alternative method in investigations of ferromagnetics because the area under the EPR absorption curve is proportional to the magnetic moment of the sample and magnetic ordering causes dramatic changes in EPR signal [34]. Our first investigations of magnetic properties of prepared multilayer nanoparticulate LB films using EPR technique pointed out to the long-range magnetic ordering of ferromagnetic type in material formed. The possibility of ferromagnetic-like ordering was confirmed by a very close behavior of EPR curves in the formed films and in control standard ferromagnetic system — a thin magnetic film of γ-Fe_2O_3 particles. The EPR

signal originated from iron in paramagnetic state was not detected and the noticeable dependence of microwave absorption at low magnetic field on the initial magnetization of the samples was observed (Fig. 7). There is a shift in the low external magnetic field region between EPR curves of nonmagnetized ferromagnetic sample and of the same sample preliminary placed in saturating external magnetic field (>0.05 Tl) due to the existence of the residual magnetic moment M and corresponding additional internal magnetic field in magnetized ferromagnetic sample [35]. As one can see in Fig. 7, the noticeable hysteresis of microwave absorption at low external magnetic field, close to that in the standard ferromagnetic system (a film of γ-Fe_2O_3), is observed in formed nanoparticulate LB films. Ferromagnetic-like behavior of EPR spectra of the nanoparticulate samples recorded in the external magnetic field generated by EPR spectrometer can correspond to superparamagnetic particles with a bound state of magnetic moments of interacting particles.

The magnetic properties of nanoparticulate LB structures formed are expected to be close to those reported for the 3-D material with ultrafine particles of the same nature. It was shown previously that the magnetic properties of 3-D polymers containing iron nanoparticles are defined ensemble of superparamagnetic particles (diameter ≈ 5 nm) and by antiferromagnetism of larger particles [36]. These magnetic properties closely resemble a spin glass below freezing temperature [36]. It is known that magnetic properties of materials with ultrafine particles consisting of transition metals with magnetic moments are temperature dependent, and also depend on the metal nature, particle structure, size and concentration in material volume. Thus, below a certain critical size, the system of intraparticle

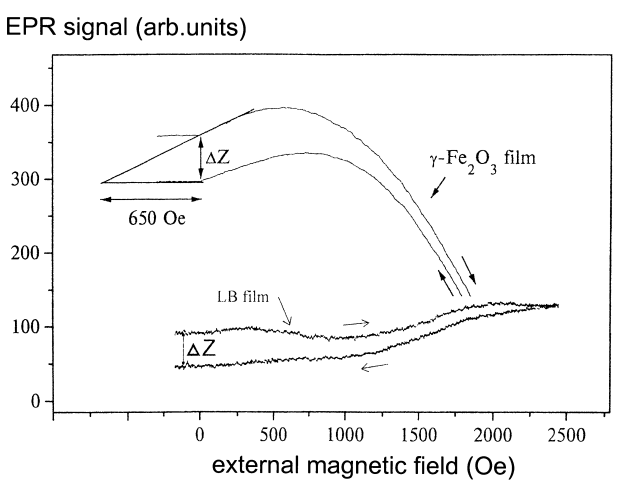

Fig. 7. Low-field hysteresis of microwave absorption (first derivative) in nanoparticulate LB film deposited by LB method ($Fe(CO)_5$/SA ratio 1:20, 10 min exposure to ultraviolet light, 50 bilayers on both sides of silicon substrate) and in magnetic film with γ-Fe_2O_3 ferromagnetic particles (thickness: 0.2–0.5 μm, saturation magnetization $I_{max} = 80$–100 G for the film as a whole; the coercive force $\Delta H = 200$–240 Oe). $T = 295$ K.

spins appeared to behave as a ferrimagnet and the particles are superparamagnetic. For amorphous alloy particles obtained by thermal decomposition of $Fe(CO)_5$, this size was about 4.5 nm at 80 K [37]. For fine particles of the same nature, the critical size at room temperature was obtained to be about 100 Å [38]. Above the critical size, there is a significant spin compensation occurring in the direction of bulk antiferromagnet at the expense of the superparamagnetic particles [38]. Superparamagnetic properties of ultrafine particles ensemble can disappear with the increase of the dipole–dipole interactions of magnetic moments of particles as a result of growth of particle size below its critical value (and corresponding increase of individual particle magnetic moment) and increase in particle concentration (decrease of distances between interacting particles). Below the definite temperature, the dipole–dipole interactions can cause the bound state of magnetic moments of interacting particles — the effect of magnetic ordering, an analog of spin-bound state in spin glasses below the spin glass freezing temperature point [39]. Due to the existence of internal magnetic field in this case, the EPR spectra of such material appears to behave as ferrimagnet or ferromagnet. This behavior corresponds to the data presented in Fig. 7.

Our results that magnetic iron nanoparticles, synthesized at the air/liquid interface, can exist in an organized chain arrangement in the deposited monolayer point out to the possibilities to create planar structures with linear chains of metal nanoparticles. The shape of synthesized particles can be varied by monolayer compression extent. Such planar material can be important for development of advanced recording media, advanced coatings with anisotropic and depth-controlled properties, nanoelectronics and other applications.

In the approach described here, there are wide possibilities to vary the conditions and to control the course of reactions involved in the interface nanoparticle formation (by variations in ultraviolet irradiation energy supply, monolayer content and compression extent, temperature, etc.). Those give possibility to control the size, shape, structure and properties of synthesized nanoparticles and to create reproducible nanostructures. The amphiphile molecules constituting the Langmuir monolayer serve also as surfactant, stabilizing the nanoparticles, and prevents reliably the aggregation of synthesized nanoparticles. The structure and properties of the nanoparticulate multilayer LB films were stable for a long time (at least a year).

4. Summary

We demonstrated the possibilities of controlled interface synthesis of ultrasmall metallic nanoparicles. Through systematic control of the ultraviolet irradiation dose and of the mixed monolayer content and compression extent, one

can manipulate the nanoparticle formation process and deposit 2-D ordered nanoparticulate structures. Different planar nanoparticulate magnetic systems can be formed by this approach. Detailed exploration of the described approach requires additional experiments addressing the questions about the structural and magnetic properties of nanoparticulate LB films. The developed approach seems as being perspective for design and creation of nanoscale functional systems (including quantum functional elements and devices) and advanced recording and nanostructured materials.

Acknowledgements

This work was supported by Russian Foundation for Basic Researches (Grants 99-03-32218 and 97-03-32199a), Russian Program on the Prospective Technologies for Nanoelectronics (Grant 96-1031).

References

[1] M.I. Shliomis, Usp. Fiz. Nauk 112 (1974) 427.
[2] Yu.A. Petrov, Clusters and Small Particles, Science, Moscow, 1986.
[3] G.B. Khomutov, E.S. Soldatov, S.P. Gubin, S.A. Yakovenko, A.S. Trifonov, A.Yu. Obidenov, V.V. Khanin, Thin Solid Films 327-329 (1998) 550.
[4] A.A. Zubilov, S.P. Gubin, A.N. Korotkov, A.G. Nikolaev, E.S. Soldatov, V.V. Khanin, G.B. Khomutov, S.A. Yakovenko, Tech. Phys. Lett. 20 (1994) 195.
[5] S.A. Iakovenko, A.S. Trifonov, E.S. Soldatov, V.V. Khanin, S.P. Gubin, G.B. Khomutov, Thin Solid Films 284–285 (1996) 873.
[6] E.S. Soldatov, V.V. Khanin, A.S. Trifonov, D.E. Presnov, S.A. Yakovenko, S.P. Gubin, V.V. Kolesov, G.B. Khomutov, JETP Lett. 64 (1996) 556.
[7] J.H. Fendler, Curr. Opin. Colloid Interface Sci. 1 (1996) 202.
[8] K.S. Mayya, V. Patil, M. Sastry, Langmuir 13 (1997) 2575.
[9] J. Yang, X.G. Peng, T.J. Li, S.F. Pan, Thin Solid Films 243 (1994) 643.
[10] T. Nakaya, Y.-J. Li, K. Shibata, J. Mater. Chem. 6 (1996) 691.
[11] J.H. Fendler, Adv. Mater. 7 (1995) 607.
[12] G.B. Khomutov, S.A. Yakovenko, T.V. Yurova, V.V. Khanin, E.S. Soldatov, Supramol. Sci. 4 (1997) 349.
[13] N.A. Kotov, M.E. Darbello Zaniquelli, F.C. Meldrum, J.H. Fendler, Langmuir 9 (1993) 3710.
[14] E.S. Smotkin, C. Lee, A.J. Bard, A. Campion, M.A. Fox, T.E. Mallouk, S.I. Webber, J.M. White, Chem. Phys. Lett. 152 (1988) 265.
[15] C. Zylberajch, A. Ruaudel-Teixier, A. Barraud, Thin Solid Films 179 (1989) 9.
[16] V. Erokhin, L. Feigin, G. Ivakin, V. Klechkovskaya, Yu. Lvov, N. Stiopina, Makromol. Chem. Makromol. Symp. 46 (1991) 359.
[17] S. Ravaine, G.E. Fanucci, C.T. Seip, J.H. Adair, D.R. Talham, Langmuir 14 (1998) 708.
[18] J.R. Thomas, J. Appl. Phys. 37 (1966) 2914.
[19] P.H. Hess, P.H. Parker, J. Appl. Polym. Sci. 1966 (1915) 10.
[20] C.H. Griffiths, M.P. O'Horo, T.W. Smith, J. Appl. Phys. 50 (1979) 7108.
[21] T.W. Smith, D. Wychick, J. Phys. Chem. 84 (1980) 1621.
[22] E. Papirer, P. Horny, H. Balard, R. Anthore, C. Petipas, A. Martinet, J. Colloid Interface Sci. 94 (1983) 220.
[23] J. van Wonterghem, S. Morup, S.W. Charles, S. Wells, J. Villadsen, Phys. Rev. Lett. 55 (1985) 410.
[24] S.R. Hoon, M. Kilner, G.J. Russel, B.K. Tanner, J. Magn. Magn. Mater. 39 (1983) 107.
[25] G.B. Khomutov, S.A. Yakovenko, E.S. Soldatov, V.V. Khanin, M.D. Nedelcheva, T.V. Yurova, Membr. Cell Biol. 10 (1997) 665.
[26] G.L. Gaines, Insoluble Monolayers at Liquid–Gas Interfaces, Wiley, New York, 1966.
[27] G.G. Roberts (Ed.), Langmuir–Blodgett Films, Plenum, New York, 1990.
[28] B. Berkovsky, M. Krakov (Eds.), Magnetic Fluids and Applications — Handbook, Begel-House, New York, 1994.
[29] D.P.E. Smith, M.D. Kirk, C.F. Quate, J. Chem. Phys. 86 (1987) 6037.
[30] S.P. Gubin, I.D. Kosobudsky, Dokl. Akad. Nauk 272 (1983) 1155.
[31] A.V. Kozinkin, V.G. Vlasenko, S.P. Gubin, A.T. Shuvaev, I.A. Dubovtsev, Inorg. Mater. 32 (1996) 376.
[32] J. van Wonterghem, S. Morup, S.W. Charles, S. Wells, J. Colloid Interface Sci. 121 (1988) 558.
[33] J.G. Simmons, J. Appl. Phys. 44 (1983) 237.
[34] R.H. Taylor, Adv. Phys. 24 (1975) 681.
[35] L.A. Blumenfeld, Yu.A. Koksharov, A.N. Tikhonov, A.I. Sherle, V.V. Promyslova, Z. Phys. Chem. 70 (1996) 884.
[36] S.P. Gubin, I.D. Kosobudsky, Usp. Khim. 52 (1983) 1350.
[37] S. Morup, B.R. Christensen, J. van Wonterghem, M.B. Madsen, S.W. Charles, S. Wells, J. Magn. Magn. Mater. 67 (1987) 249.
[38] L.N. Mulay, D.W. Collins, A.W. Thompson, P.L. Walker Jr., J. Organomet. Chem. 178 (1979) 217.
[39] V.V. Kokorin, A.E. Perekos, JETF Lett. 27 (1978) 500.